

### **Additional experimental details:**

All manipulations were carried out under atmospheric conditions, unless otherwise mentioned. All reagents were purchased from commercial sources and used without further purification. Millipore deionized water 18.2 M $\Omega$  was used to prepare all the solutions. All electrochemical measurements were done using an Autolab potentiostat/galvanostat.

A three-electrode configuration under front-side simulated AM 1.5 G solar illumination was used for photoelectrochemical hydrogen evolution measurements. Pt wire was used as the counter electrode and an Ag/AgCl (KCl sat.) electrode was used as the reference electrode. Different electrolyte buffer solutions were used at different pH values and were referenced in the text by the pH value unless otherwise mentioned. 1.0 M KOH (Merck) solution was used as pH 13.6 electrolyte and 1.0 M H<sub>2</sub>SO<sub>4</sub> (Merck, 95–97%) was used as pH 0. The pH 4.0 solution consists of 1.0 M potassium hydrogen phosphate (Sigma, >99.0%) buffer. The pH 7.0 solution consists of a 1.0 M Na<sub>2</sub>SO<sub>4</sub> (Sial, 99+%). The pH 9.0 solution consists of 0.1 M sodium tetraborate (Sial, 99.5+%). The photoresponse was measured under irradiation from a 450-W Xe lamp (Osram) equipped with a KG3 filter (3 mm, Schott, filters ultraviolet and infrared light), calibrated with a Si diode to simulate AM 1.5 G illumination (1 sun) between wavelengths of 300 and 800 nm. Photocurrent stability tests were carried out by measuring the photocurrent produced under constant light irradiation at a fixed electrode potential of 0 V versus RHE under continuous nitrogen bubbling. Faradaic efficiencies were measured in a gastight, home-made H cell calibrated for pressure and gas quantification previously reported.<sup>[1-2]</sup> The Ni-Mo catalyst loading on FTO was estimated using the modified anodic stripping voltammetry technique previously reported by Mckone *et al.*<sup>[3]</sup> The deposition charge efficiency can be determined by integrating the charges passed during anodic stripping of the Ni-Mo catalyst immersed in 1.0 M H<sub>2</sub>SO<sub>4</sub> and comparing this value to the total charges passed during electrodeposition of the catalyst. This gives a lower limit due to the fast dissolution of the catalyst in acid that is not coupled to electron transfer from the electrode.

The photoelectrodes were characterized by High Resolution SEM and XPS. High resolution SEM images were taken using a Zeiss MERLIN Microscope. ImageJ software was used to measure the distances in SEM images. XPS data were collected on an Axis Ultra instrument (Kratos Analytical) under ultrahigh vacuum (<10<sup>-8</sup> torr) using a monochromatic Al K $\alpha$  X-ray source (1,486.6 eV), in the Surface Analysis Laboratory of Interdisciplinary Center for Electron Microscopy at École Polytechnique Fédérale de Lausanne. The source power was maintained at 150 W (10 mA, 15 kV). The adventitious carbon 1s peak was calibrated at 284.8 eV and used as an internal standard to compensate for any charging effects. Both

curve fitting of the spectra and quantification were carried out with the CasaXPS software using relative sensitivity factors from the supplier.

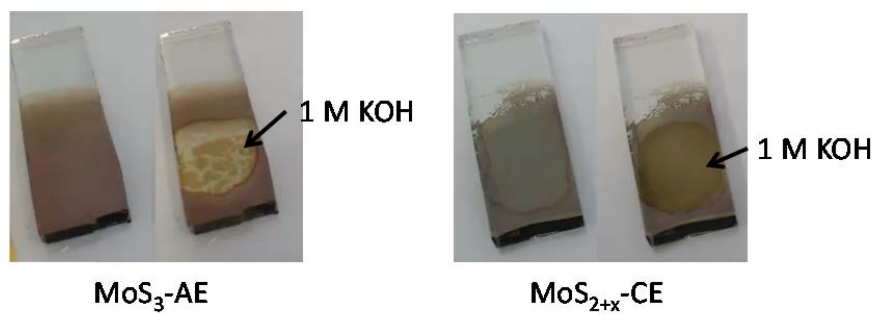


**Figure S1.** Images showing the morphological changes of different MoS<sub>2+x</sub> electrodes after contact with a 1 M KOH solution. The MoS<sub>3</sub>-AE film refers to a film made by anodic electrolysis and contains mainly MoS<sub>3</sub>; MoS<sub>2+x</sub>-CE film refers to a film made by cathodic electrolysis and contains already the active MoS<sub>2+x</sub> catalyst.

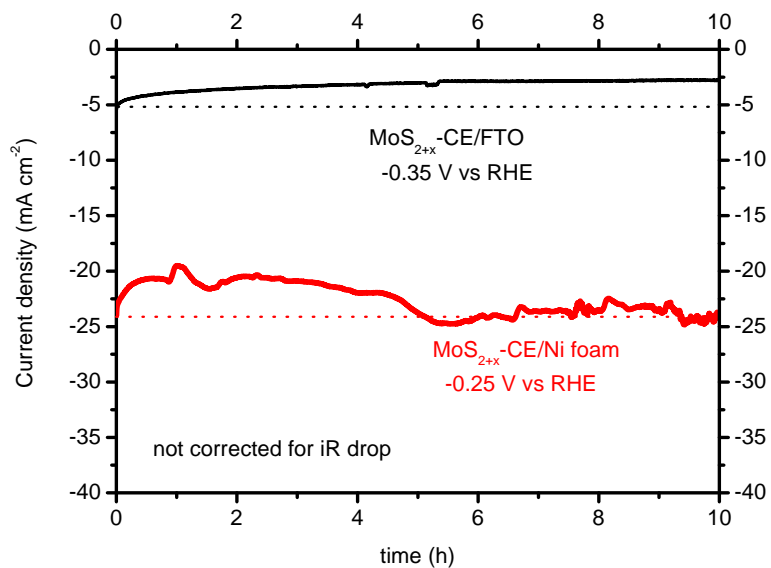


**Figure S2.** Potentiostatic electrolysis in 1 M KOH. The data were not corrected for iR drop. Dotted lines correspond to the initial current density and have been added to guide the eye. The catalyst film deposited on FTO retains 54% of its initial current density after 10 h. Deactivation of the catalysts on the flat films is probably due to mechanical stress caused by H<sub>2</sub> bubble formation and can be alleviated by using porous conductive substrates. The MoS<sub>2+x</sub>-CE/Ni foam retains close to 100% of its initial current density after ten hours. This observation is in agreement with the results obtained by Laursen *et al.* for electrochemical hydrogen evolution using amorphous molybdenum sulfide films electrodeposited on FTO and high-porosity carbon paper substrates at pH 0 in 1 M HClO<sub>4</sub>.<sup>[4]</sup>

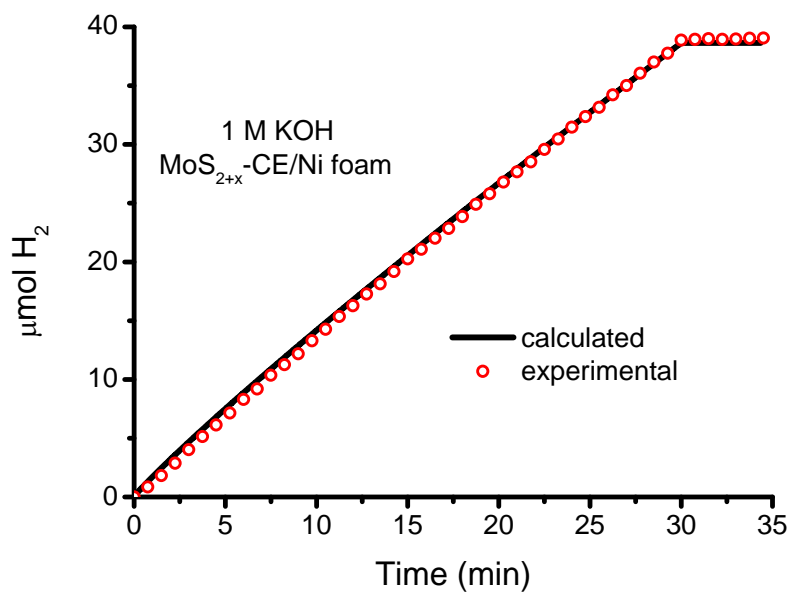


**Figure S3.** Faradaic efficiency of hydrogen evolution for a MoS<sub>2+x</sub>-CE/Ni foam electrode at 200 mV overpotential in 1 M KOH.

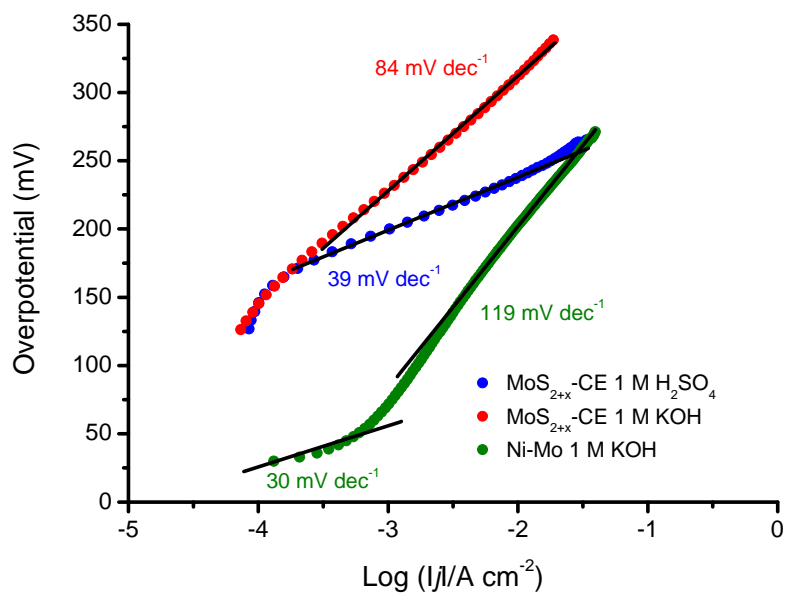
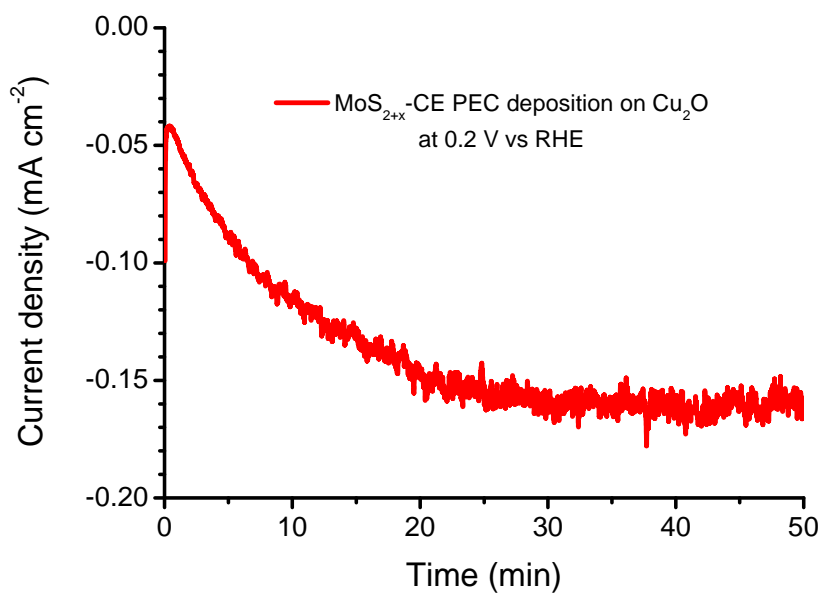


**Figure S4.** Tafel slopes for HER determined from the iR drop corrected linear sweep voltammetry curves. Conditions: 1 M KOH, scan rate = 1 mV s<sup>-1</sup>.

a)



b)

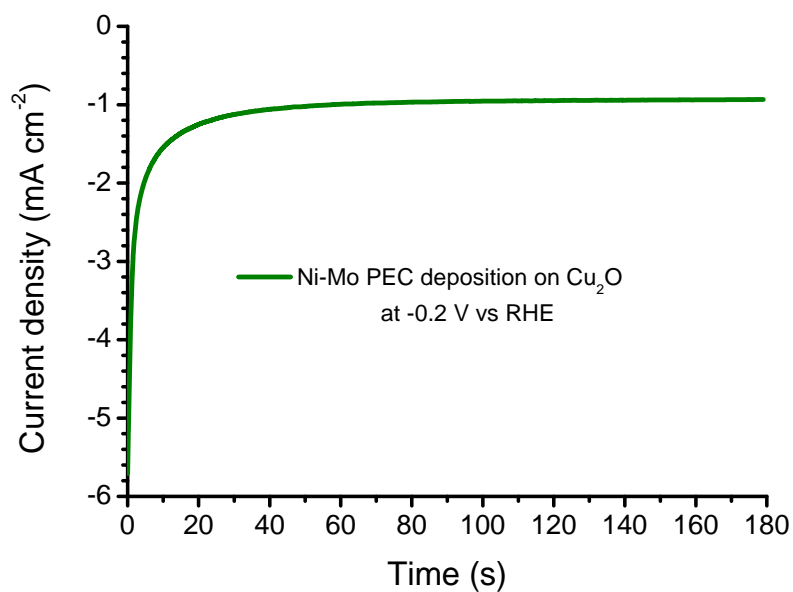
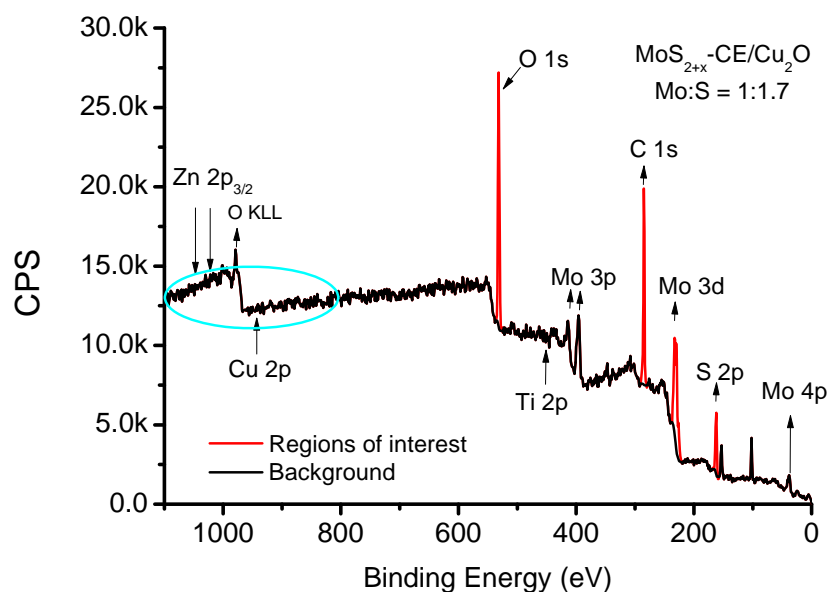


**Figure S5.** Current-time curve during photoelectrochemical deposition of a) MoS<sub>2+x</sub>-CE and b) Ni-Mo HER catalysts on surface protected Cu<sub>2</sub>O under simulated AM 1.5 illumination (1 sun).

a)



b)

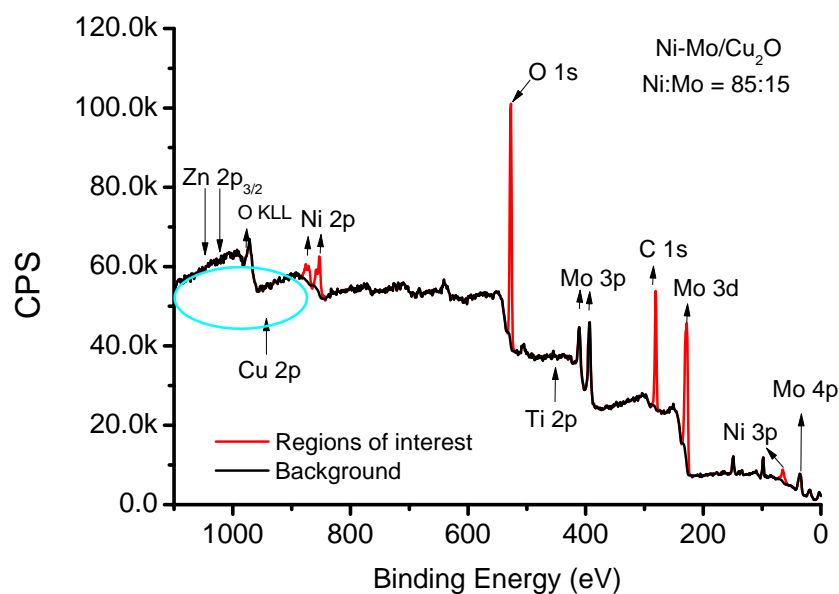


**Figure S6.** XPS survey spectra of as-deposited a)  $\text{MoS}_{2+x}\text{-CE/Cu}_2\text{O}$  and b)  $\text{Ni-Mo/Cu}_2\text{O}$  photocathodes. The absence of any Ti 2p or Cu 2p signals indicate the conformal coating of the surface protected  $\text{Cu}_2\text{O}$  photocathode. The signals at binding energies of 99 and 151 eV correspond to Si 2p and Si 2s, respectively. The Si signal arises from the holt-melt used to surround the active area of the photocathode during catalyst deposition.



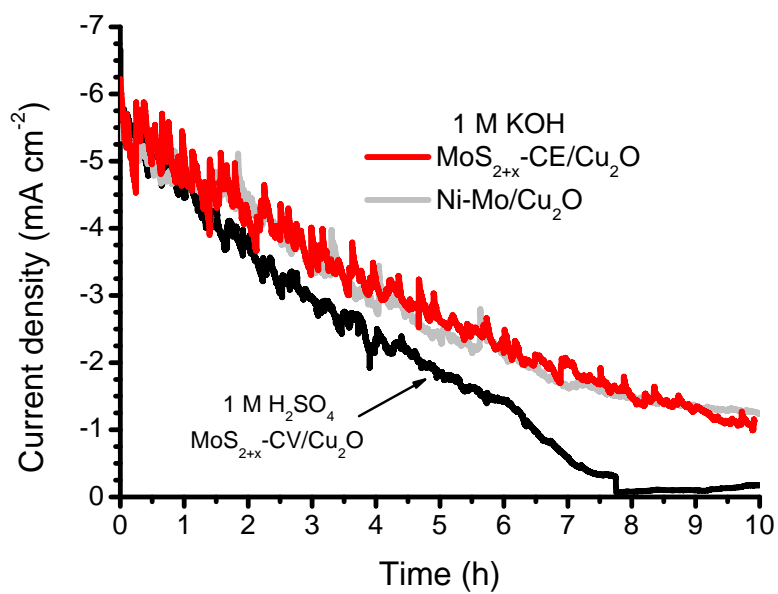


**Figure S7.** PEC Stability during HER for MoS<sub>2+x</sub>/Cu<sub>2</sub>O and Ni-Mo/Cu<sub>2</sub>O photocathodes. Conditions: AM 1.5 illumination (1 sun), continuous nitrogen bubbling, biased at 0V vs. RHE.

**Table S1.** Comparison of HER activity of various Earth-abundant catalysts in alkaline solutions

Catalyst	Loading (mg cm <sup>-2</sup> )	Electrolyte	Current density (mA cm <sup>-2</sup> )	Overpotential (mV)	Reference
Ni <sub>2</sub> P	1.0	1 M KOH	20	205	Popczun <i>et al.</i> <sup>[5]</sup>
Ni <sub>2</sub> P	0.38	1 M KOH	20	250	Feng <i>et al.</i> <sup>[6]</sup>
Ni	-	1 M KOH	20	320	Feng <i>et al.</i> <sup>[6]</sup>
Ni(OH) <sub>2</sub>	0.4	1 M KOH	20	300	Feng <i>et al.</i> <sup>[6]</sup>
Mo <sub>2</sub> C	0.8	1 M KOH	20	210	Vrubel <i>et al.</i> <sup>[11]</sup>
MoB	2.3	1 M KOH	20	240	Vrubel <i>et al.</i> <sup>[11]</sup>
Ni-Mo nanopowder	1.0 13.4	2 M KOH	20 130	70 100	McKone <i>et al.</i> <sup>[7]</sup>
MoS <sub>2+x</sub> /FTO	0.02	1M KOH	10	310	This work
Ni-Mo/FTO	0.012	1M KOH	10	200	This work
MoS <sub>2+x</sub> /Ni foam	-	1 M KOH	10	210	This work
			20	240	
			100	335	
Ni-Mo/Ni-foam	-	1M KOH	10	150	This work
			20	195	
			100	280	

- [1] H. Vrubel, X. Hu, *Angew. Chem. Int. Ed.* **2012**, *51*, 12703-12706.
- [2] C. G. Morales-Guio, S. D. Tilley, H. Vrubel, M. Gratzel, X. Hu, *Nat. Commun.* **2014**, *5*, 3059.
- [3] J. R. McKone, E. L. Warren, M. J. Bierman, S. W. Boettcher, B. S. Brunschwig, N. S. Lewis, H. B. Gray, *Energy Environ. Sci.* **2011**, *4*, 3573-3583.
- [4] A. B. Laursen, P. C. K. Vesborg, I. Chorkendorff, *Chem. Commun.* **2013**, *49*, 4965-4967.
- [5] E. J. Popczun, J. R. McKone, C. G. Read, A. J. Biacchi, A. M. Wiltrout, N. S. Lewis, R. E. Schaak, *J. Am. Chem. Soc.* **2013**, *135*, 9267-9270.
- [6] L. Feng, H. Vrubel, M. Bensimon, X. Hu, *Phys. Chem. Chem. Phys.* **2014**, *16*, 5917-5921.
- [7] J. R. McKone, B. F. Sadler, C. A. Werlang, N. S. Lewis, H. B. Gray, *ACS catal.* **2013**, *3*, 166-169.